Carbohydrate Polymers 153 (2016) 160–168

Contents lists available at ScienceDirect

Carbohydrate Polymers

journal homepage: www.elsevier.com/locate/carbpol

Bioreducible PEI-functionalized glycol chitosan: A novel gene vector with reduced cytotoxicity and improved transfection efficiency

Shahrouz Taranejoo[a,b], Ramya Chandrasekaran[a], Wenlong Cheng[a], Kerry Hourigan[c,*]

[a] Department of Chemical Engineering, Faculty of Engineering, Monash University, Melbourne, VIC 3800, Australia
[b] Harvard-MIT Division of Health Sciences and Technology, Massachusetts Institute of Technology, Cambridge, MA 02139, USA
[c] Laboratory for Biomedical Engineering/Fluids Laboratory for Aeronautical and Industrial Research, Department of Mechanical and Aerospace Engineering, Faculty of Engineering, Monash University, Melbourne, VIC 3800, Australia

ARTICLE INFO

Article history:
Received 13 January 2016
Received in revised form 10 July 2016
Accepted 19 July 2016
Available online 21 July 2016

Keywords:
GCS-ss-PEI
Glycol chitosan
PEI
Redox-responsive
Non-viral vector
Cytotoxicity

ABSTRACT

Non-viral gene delivery has been well recognised as a potential way to address the main safety limitations of viral gene carriers. A new redox-responsive PEI derivative was designed, synthesized and evaluated for non-viral delivery applications of GFP DNA. Glycol chitosan was covalently attached to highly branched LMW PEI via bio-cleavable disulfide bonds to synthesize a new redox-responsive gene carrier (GCS-ss-PEI). Results showed the enhanced buffering capacity of GCS-ss-PEI, 43.1%, compared to the buffering capacities of both LMW PEI and HMW PEI, 23.2% and 31.5%, respectively, indicating more likely endosomal escape of the entrapped gene for GCS-ss-PEI. Moreover, electrophoretic gel retardation assay, performed to investigate the binding strength of GCS-ss-PEI to GFP DNA, showed stronger complexation with GFP DNA in GCS-ss-PEI at non-GSH condition. Employing GCS and incorporation of disulfide bonds in the structure of the PEI-based gene carrier resulted in improved redox-responsivity, reduced toxicity, enhanced endosomal escape and GFP DNA transfection. The facilitated intracellular gene release along with excellent redox-responsive characteristics and dropped cytotoxicity suggests the potential of GCS-ss-PEI as a candidate for developing highly efficient and safe gene vectors.

1. Introduction

Gene therapy has attracted a great deal of interest in medicine due to its potential to treat acquired and inherited diseases at their genetic roots. Gene therapy continues to encounter some obstacles, however, including the difficulty of transferring genes through intricate cellular and tissue barriers (Li, Wei, & Gong, 2015; L.M. Li et al., 2015; Naldini, 2015). As such, creating safe and effective delivery vectors is important for advancing gene therapy (Yin et al., 2014). Recently, non-viral gene delivery systems have been employed to address the challenges presented by viral delivery systems, e.g., carcinogenesis, immunogenicity, limited gene-carrying capacity and difficulty of mass vector production (Lai, 2015; Patnaik & Gupta, 2013; Yin et al., 2014). Non-viral nanoparticles can protect genes before reaching genes at the site of action, and against degradation by endonucleases in physiological fluids and the extracellular space. This gene protection is crucial to improving circulation time and intracellular transfection efficiency (Xiaoxiao et al., 2015; Ragusa, García, & PenadÉs, 2007; Yin et al., 2014).

Polyethyleneimine (PEI) derivatives were introduced as a novel class of gene vectors with high gene carrying capacity and the ability to protect DNA against extracellular degradation. However, in spite of the high gene complexation of commercial PEI, there are two main barriers: high immune system response and a high level of cellular toxicity. The toxicity is mainly due to its cationic nature and a noncleavable molecular structure that restricts its biomedical applications (L. Li et al., 2015; L.M. Li et al., 2015; Patnaik & Gupta, 2013; Ragusa et al., 2007; Taranejoo, Liu, Verma, & Hourigan, 2015; Zhang et al., 2013).

Specifically, chitosan has already been widely used in gene and drug delivery systems (Alamdarnejad et al., 2013; Taghizadeh et al., 2015). Glycol chitosan (GCS) is a soluble derivative of chitosan with series of outstanding characteristics such as hydrophilicity, biodegradability, excellent tumor-homing efficacy due to the long blood circulation, low immunogenicity along with acceptable cellular and tissue internalization that make GCS a potential candidate for the delivery of therapeutic agents (Kim et al., 2008; Mitra et al., 2014).

* Corresponding author.
E-mail addresses: Kerry.hourigan@monash.edu, kerry.hourigan@gmail.com (K. Hourigan).

http://dx.doi.org/10.1016/j.carbpol.2016.07.080
0144-8617/

Moreover, GCS, unlike chitosan, can retain a positive charge even at physiological pH value (Makhlof, Werle, Tozuka, & Takeuchi, 2010). However, the application of GCS as a gene vector may be restricted by its lower amino group density, which in comparison with PEI decreased DNA condensation capacity. In this study, we formulated and developed a novel gene carrier, a glycol chitosan-based disulfide-containing polyethylenimine derivative (GCS-ss-PEI), by grafting glycol chitosan (GCS) into branched low molecular weight polyethyleneimine (LMW PEI) via cleavable disulfide bonds. Employing highly-branched PEI, compared to linear PEI, can create stronger and smaller polyplexes with DNA (Goula et al., 1998; Wightman et al., 2001). GCS-ss-PEI performance as a potential non-viral gene vector was examined by evaluating its DNA binding capacity, polymer toxicity, redox-responsive characteristics and gene transfection efficiency.

2. Materials and methods

2.1. Materials

Glycol chitosan (DS: 60% (titration), molecular weight 250 kD, crystalline), 3,3-dithiodipropionic acid (DTDP), 3-(4, 5-dimethylthiazol-2-yl)-2,5-diphenyltetrazolium bromide (MTT), dimethylaminopyridine (DMAP), Triethylamine (TEA), dimethyl sulfoxide (DMSO), 1-ethyl-3-(3-dimethylaminopropyl), acetyl chloride, carbodiimide hydrochloride (EDC), *N*-hydroxysuccinimide (NHS), Fluorescein isothiocyanate isomer (FITC), heparin, and glutathione (GSH) were purchased from Sigma Co., Ltd. (USA). Low molecular weight branched polyethylenimine (LMW PEI, Linear, MW 2500) and high molecular weight branched polyethylenimine (HMW PEI, branched, MW 25,000) were supplied from Polyscience Co. LysoView™ 633 was purchased from Biotium, Inc.(USA). Lipofectamine® 2000 was supplied from Thermofisher Co., (USA). *DNA plasmid encoding green fluorescent protein* (GFP DNA) was extracted and purified from E-coli bacterial colonies using the Qiagen miniprep kit as previously described elsewhere (Zhang & Cahalan, 2007).

2.2. Synthesis of GCS-ss-PEI

DTDP (2 g) was added to 20 ml of acetyl chloride and then refluxed at 65 °C for 2 h. After evaporation of the solvent under vacuum, the remaining was precipitated and washed twice by diethyl ether. The product, DTDPA, was dried with N_2 gas at room temperature. A mixture of 50 mg DMAP (0.4 mmol) and 384 mg of the obtained DTDPA (2 mmol) was added to dried DMF (10 ml) and then added droplet by droplet into 10 ml of GCS aqueous solution (10 mg/ml). After dissolving the materials, 40 mg TEA (0.4 mmol) was added to the mixture and the solution was stirred for 12 h at ambient temperature.

The obtained dispersion was dialyzed against water and DMF (MWCO: 3500) for two days and then was dried with N_2 gas at room temperature to obtain GCS-ss-COOH. To synthesize GCS-ss-PEI, GCS-ss-COOH was activated with EDC and sulfo-NHS reagents, and then reacted through carbodiimide crosslinking with amino groups of LMW PEI. Briefly, 230 mg NHS (2 mmol) and 383.3 mg EDC (2 mmol) was added to 10 ml of GCS-ss-COOH aqueous solution (10 mg/ml) and then was stirred for 1 h at room temperature. Subsequently, the above mixture was added to 20 ml of LMW PEI aqueous solution (1%) and stirred for 2 days. The product was dialyzed with millipore water for 3 days (MWCO: 3500), followed by freeze-drying for 2 days to achieve GCS-SS-PEI.

2.3. Fourier transform infrared (FTIR) spectroscopy

The FTIR spectra of glycol chitosan, PEI and GCS-ss-PEI were recorded using an attenuated total reflectance (ATR) Fourier transform infrared (FTIR) (PerkinElmer, USA) in the range of 500–4000 cm^{-1} at an average of 40 scans with a resolution of 4 cm^{-1} over the spectral region 4000–500 cm^{-1}.

2.4. Buffering capacity

The buffering capacity of the polymers was calculated as the percentage of amino groups that were protonated from pH 7.4–5.1 (Jia et al., 2013).

An acidic titration procedure, over a pH dropping range of 11–4, was performed to determine the buffering capacities of LMW PEI, HMW PEI and GCS-ss-PEI. Polymers (0.1 mmol nitrogen atoms) were dissolved in 2.0 ml of 10 mM NaCl and dialyzed against 10 mM NaCl for 3 days using 800 MW cutoff dialysis membrane. NaOH solution at 0.2 mmol was added droplet by droplet to increase the solution pH to 11. HCl solution 0.1 M was added to the polymer solution in increments of 20 μl. At each increment of HCl addition, pH was measured. The following equation was employed to calculate the buffering capacity.

$$\text{The buffer capacity } (\%) = \frac{\delta HCl \times 0.1\text{M}}{N_{\text{amino}}\,(\text{mmol})} \times 100 \quad (1)$$

Here, δHCl is the required volume of HCl solution (mL) for changing the pH value of Polymer solution from 7.4 to 5.1. N (mmol) is the total number of moles of polymer amines in each titration.

2.5. Cell culture

Human embryonic kidney (HEK) cells were originally derived from human embryonic kidney cells grown in tissue culture. The cells were cultured in growth DMEM medium (supplemented with 10% FBS and 100 U mL of penicillin antibiotics). Cell culture was performed in incubators maintained at 37 °C with 5% CO2 under fully humidified conditions. All experiments were done on cells with a maximum 70% of confluence.

2.6. Cytotoxicity assay of GCS-ss-PEI

HEK 293T (4000 cells/well) was seeded in 96-well plates for 1 day and then incubated with 200 μl of complete DMEM containing LMW PEI, HMW PEI, or GCS-ss-PEI at different concentrations. After 4 h of incubation, the medium in each well was replaced with 180 μl of fresh complete medium and cells were cultured for 24 h. Then 20 μl of MTT solution in PBS (5 mg/ml) was added to each well and cells were incubated for another 6 h. After removing the spent medium, 150 μl DMSO was added into each well to dissolve purple formazan crystals formed after reducing the yellow tetrazolium salt (MTT).

The optical intensity for each well was measured at 570 nm using a microplate reader (model 550, BioRad Lab, Hercules, CA).

2.7. Formation of GCS-ss-PEI/DNA polyplexes

For each experiment, the complexes of CS-ss-PEI and DNA were freshly prepared at different N/P ratios by mixing equal volumes of sterilized aqueous solution of copolymer and DNA stock diluted with deionized water. After vortexing for 30 s, the mixture was placed in a shaker incubator for 30 min at room temperature to complete the formation of the polyplexes.

2.8. Size, zeta potential and morphological studies

The size and surface charges (ζ potential) of the complexes were measured by dynamic light scattering (DLS) at 25 °C, with a Zetasizer Nano ZS with a 633 nm laser (Malvern, UK) as previously described (Jia et al., 2013). The morphology of the complexes was observed by scanning electron microscopy (Magellan 400 FEGSEM, an extreme high resolution (XHR) instrument equipped with a monochromator allowing improved resolution at low accelerating voltages). After preparing polyplexes at different (N/P) ratios, 20 μl of each polyplex solution was carefully dropped on a clean silica wafer. The samples were dried by N_2 gas at room temperature. Then, the samples were sputter coated by an ultra-thin layer of Pt (2 nm) before imaging.

2.9. DNA binding efficiency

The DNA binding efficiency of HMW PEI and GCS-ss-PEI was investigated by gel electrophoresis. Solutions of polyplexes with different N/P ratios (including 0.2 ng of DNA) were loaded into Agarose gel (1.0%) containing ethidium bromide (0.5 μg/m1) prepared in TAE buffer. Gel electrophoresis was run at 120 V for 30 min. The DNA banding results were visualized by Bio-Rad Molecular Imager UV light.

2.10. Redox-responsive characteristics

To assess the reduction sensitivity of the complexes, an appropriate amount of 10 mm GSH in the presence of heparin (1 μl) was added to each polyplex solution (different N/P ratio). The solutions were incubated at 37 °C with constant shaking for 120 min before measurement. Gel electrophoresis was used to determine the amount of DNA facilitated release as previously described. The GSH concentration (10 mM) mimics an intracellular environment and a small amount of heparin was used to signify the visibility of the DNA bands.

2.11. In vitro gene transfection

DNA plasmid encoding green fluorescent protein (GFP DNA) was used as a model gene for transfection experiments to HEK 293 cells. The cells were plated in 24-well plates (6×10^5 cells per well) in growth DMEM medium (supplemented with 10% FBS and 100 U mL of penicillin antibiotics). After reaching 70% of confluence, the cells were rinsed with PBS buffer and re-incubated with 200 μl of polyplex dispersion (1 μg of GFP DNA per well) and 400 μl of the transfection culture medium (without FBS) at 37 °C. After 6 h, culture medium containing remained polyplexes was removed, 600 μl of growth culture medium was added, and the cells were cultured for 48 h. Investigation of the cells was conducted using fluorescence microscope (OLYMPUS, IX 71, Japan). The cells were collected and then a flow cytometer (BD FACSCalibur™, Cell Analyzer, BD Biosciences) was used to quantify the transfection efficiency of GFP DNA into the cells. The HMW PEI/GFP DNA polyplex (optimalN/P ratio of 10) was used as a reference.

2.12. FITC conjugation of high molecular weight PEI and GC-PEI for confocal imaging

HMW PEI and GCS-ss-PEI solutions were prepared by dissolving them in PBS (20 mg/ml). FITC was dissolved in DMSO for a final concentration of 10 mM. To 500 μl of HMW PEI and GCS-ss-PEI, 50 μl of FITC was added and the reaction mixture was left to react at 18 °C for 2.5 h. The final FITC-PEI and FITC-GCS-ss-PEI were dialyzed (MWCO 3500) against 50 ml of ice cold PBS to remove the excess FITC.

2.13. Endosomal escape

HEK 293T cells were seeded on 24 well plate at a population of 12,000 per well. The plate was incubated overnight at 37 °C in CO2 incubator. To the cells, 60 μl of FITC-HMW PEI and FITC-GCS-ss-PEI were added and incubated again with the transfection medium OptiMEM for 6 h. After 6 h, the cells were washed twice with 1 ml PBS to remove the OptiMEM medium and cells were stained first with LysoView 633 for visualizing lysosomes under UV. For this staining, 10 μl of 100 M LysoView™ was dissolved in 10 ml of complete MEM and to each well, 500 μl was added and incubated for 5 min at 37 °C. Then, cells were washed twice with 1 ml PBS and stained for nucleus visualization using DAPI. For this staining, 50 μl of 10 M DAPI was dissolved in 5 ml of PBS and 200 μl was added to each well, incubated for 5 min at 37 °C and washed again with PBS. When cells were fixed with 4% Paraformaldehyde, a decrease in LysoView™ fluorescence was observed. Hence, the cells were imaged live using a confocal microscope at 40× magnification.

2.14. Statistical analysis

Statistical analysis was done using the Excel program version 2010. The obtained results were expressed as mean ± standard deviation (SD). Statistical differences between the groups of data were analyzed by Student's *t*-test. Differences were considered significant for probability values of $P < 0.05$.

3. Results and discussion

3.1. Characterization of GCS-ss-PEI

Fig. 1 shows a schematic of the synthesizing procedure for GCS-ss-PEI. Instead of linear PEI, branched LMW PEI was employed to form the structure of GCS-ss-PEI due to its stronger complexation with DNA, which typically results in smaller complexes (Feng et al., 2014; Wightman et al., 2001). GCS was used a soluble derivative of chitosan with lower toxicity and reduced solution viscosity. Employing dehydrated DTDP (DTDPA) in combination with GCS was considered as an effective approach to prevent unwanted reactions between GCS molecules. This synthesizing procedure was designed to limit the construction of disulfide bonds only between GCS and LMW PEI molecules. Moreover, small amounts of DMAP and TEA were used to partially activate the carboxyl group of GCS (Moyuan et al., 2012; Yue, Wu, Liu, Zhao, & Lu, 2015). The activation of a portion of the carboxyl groups of GCS was done to create disulfide bonds with amino groups of LMW PEI. This was aimed at releasing some amino groups of GCS with the ability to retain a positive charge at physiological pH values so as to effectively participate in DNA condensation (Makhlof et al., 2010).

The chemical structures of PEI, GCS and GCS-ss-PEI were identified with Fourier transformation infrared spectroscopy (FITR) and the results are shown in Fig. 2. The bonds at 1052 and 1038 are fingerprints of the glycosidic linkages in GCS and GCS-ss-PEI, respectively (Inbaraj, Tsai, & Chen, 2012). Characteristic peaks of PEI at 3268 cm^{-1} (—N—H stretching), 2882 cm^{-1} (—C—H stretching) were shifted into lower energy bonds, 3244 cm-1, 2830 cm-1 and 2788 cm-1, respectively (Wang, Liu, Nie, Wei, & Cui, 2013). These shifts imply an interaction between GCS and amino groups of PEI. The bonds at 1660 cm^{-1} and 1549 cm^{-1} of GCS can be attributed to the adsorption of —(—C═O—)— and (—N—H—) of the —CONH— group. Around these regions, the same bonds with significantly enhanced strength were found, indicating the grafting of the disulfide crosslinker on the GCS. The curve at 1463 cm^{-1} and the strong bond at 1398 cm^{-1} can be ascribed to the amplified absorption of

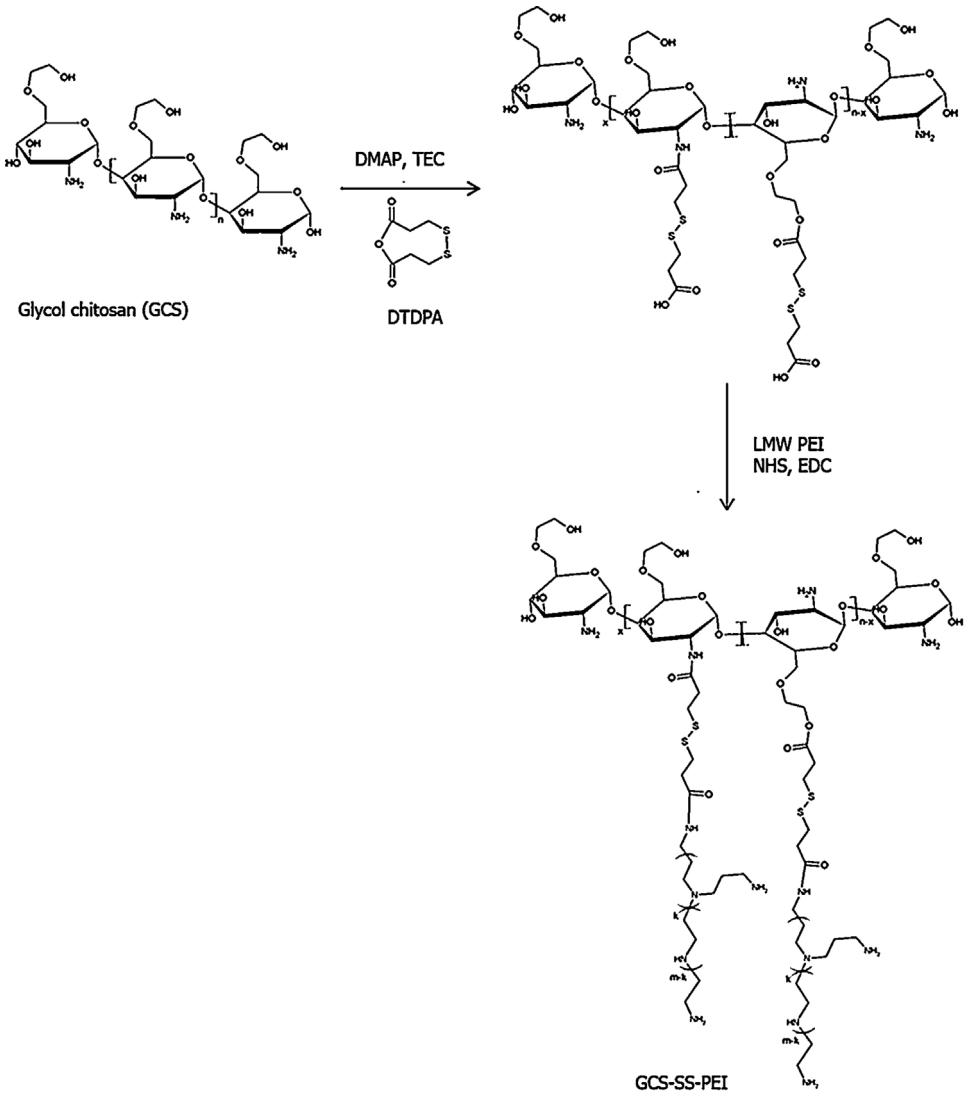

Fig. 1. Synthesis of GCS-ss-PEI.

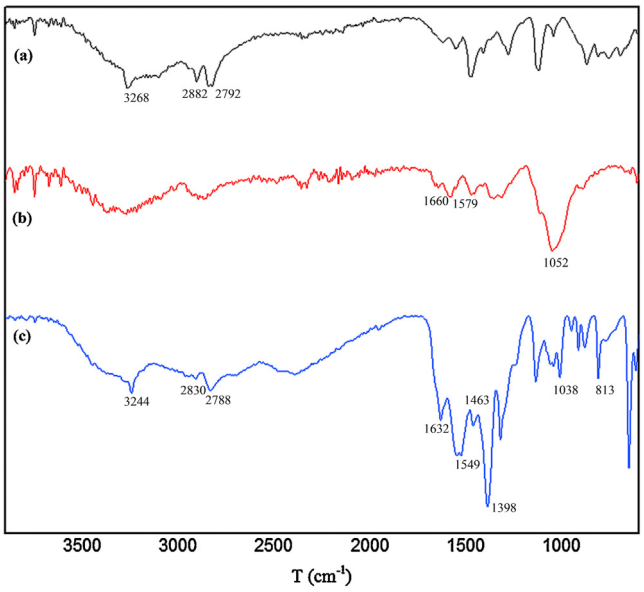

Fig. 2. The FTIR spectra of PEI (a), GCS (b) and GCS-ss-PEI (c).

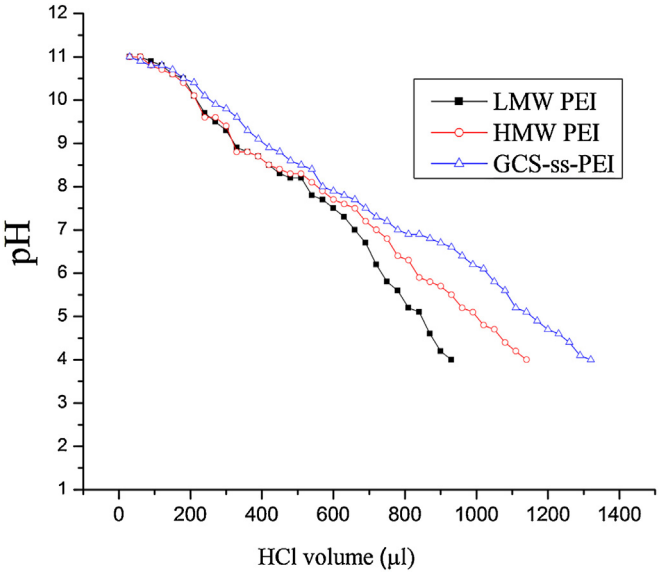

Fig. 3. Buffering capacity of the of LMW PEI, HMW PEI and GCS-ss-PEI polymers.

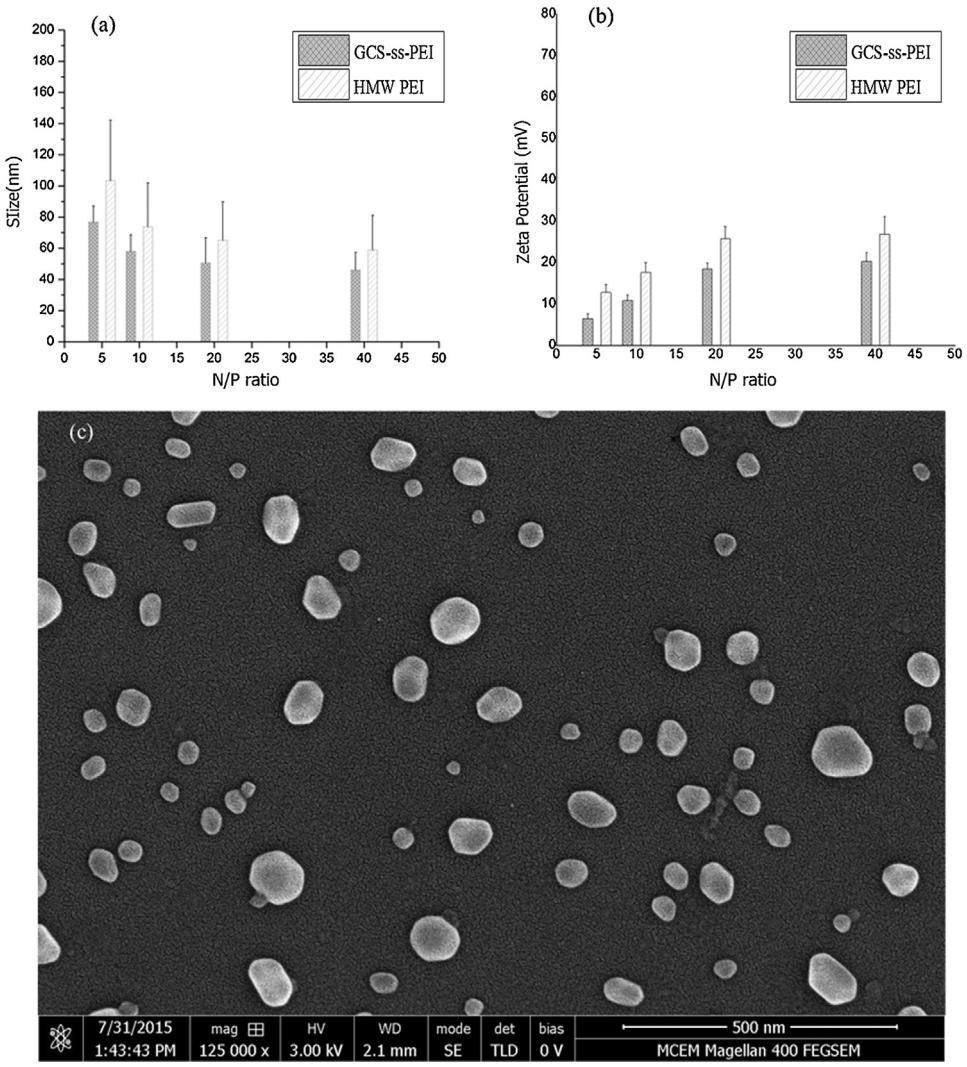

Fig. 4. (a) Particle size and (b) zeta-potential of polyplexes fabricated from GCS-ss-PEI and HMW-PEI with DNA at various N/P ratios ranging from 1 to 40. (c) SEM microimage of GCS-ss-PEI/DNA polyplex at N/P ratio of 20.

the $-CH_2CH_2NH-$ moiety of PEI in GCS-ss-PEI (Jia et al., 2013). The yield of the reaction obtained was 54%.

Fig. 3 shows the buffering capacity of the of LMW PEI, HMW PEI and GCS-ss-PEI polymers. A higher buffering capacity was attributed to more acid required to protonate amino-groups of polymers. Increasing the buffering capacity results in enhanced endosomal escape (El-Sayed, Futaki, & Harashima, 2009). The endosomal microenvironment was acidified (pH 5–6) by membrane-bound proton-pump ATPases. This microenvironment, followed by further acidified lysosomes microenvironments, promotes the degradation rate of the genes. Hence, escape from endosome to cytosol is required to enhance gene transfection efficiency. The positively charged amine groups of the catiomers facilitate endosomal escape through their specific action, which is known as a proton sponge effect (Dominska & Dykxhoorn, 2010). As shown, the buffering capacity of GCS-ss-PEI, 43.1% ($P < 0.001$), was

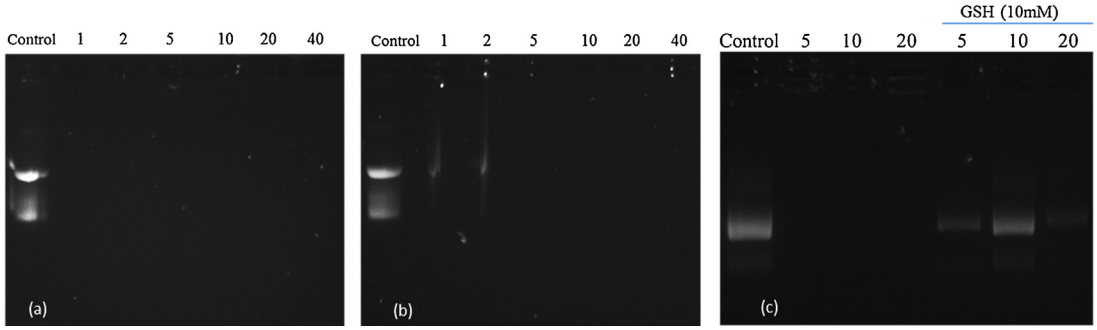

Fig. 5. Gel electrophoresis results of polyplexes at N/P ratios of 5–20; Binding strength of (a) GCS-ss-PEI/DNA, (b) HMW PEI/DNA. (c) redox-responsive destabilization of polyplexes and GSH-induced gene release for GCS-ss-PEI/DNA.

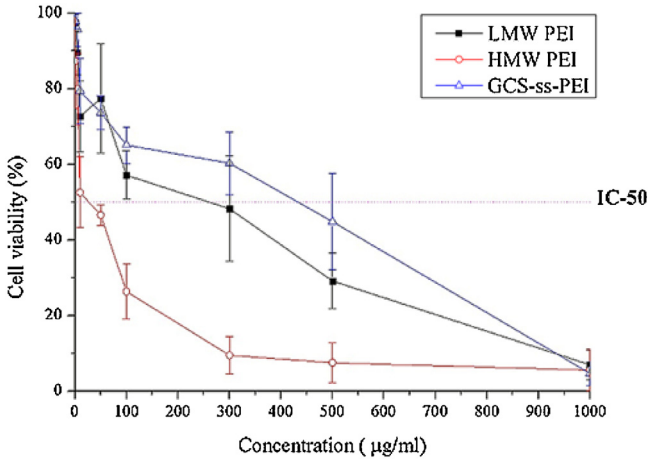

Fig. 6. Cytotoxicity of LMW PEI, HMW PEI and GCS-ss-PEI at various N/P ratios in HEK 293T cells by MTT assay.

greater than the buffering capacities of both LMW PEI ($P < 0.001$) and HMW PEI ($P < 0.05$), at 23.2% and 31.5%, respectively. This result probably relates to the difference between the ionization behavior of chitosan and PE that makes the buffering capacity of a chitosan derivative higher than that of PEI. The higher buffering capacity indicates possible higher rates of endosomal escape for GCS-ss-PEI (Richard, Thibault, De Crescenzo, Buschmann, & Lavertu, 2013).

3.2. Characterization of GCS-ss-PEI/DNA complexes

Fig. 4 shows the sizes and zeta-potentials of the polyplexes with different N/P ratios. The size of GCS-ss-PEI/DNA was between 50 and 90 nm. The largest nanoparticles (average size 81.2 and 106.4 for GCS-ss-PEI/DNA and HMW PEI/DNA, respectively) were found when the N/P ratio was 5/1. These nanoparticles are quite small. Such small particles (with a typical range of 10–100 nm in diameter) can be taken up at the cell surface and transferred to the nucleus during a short period of time (Cai, Conley, & Naash, 2008).

The same conditions resulted in formation of nanoparticles with the least amount of surface positive charge. No significant change in Zeta potential was found when increasing the N/P ratio from 20 to 40, indicating the saturation of the nanoparticles with DNA. In regard to previous articles, the decreased charge density of GCS-ss-PEI, at the same N/P ratio, may result in reduced immunogenicity and enhanced circulation time (Lu, Dai, Lv, & Zhao, 2014; Mitra et al., 2014; Taranejoo et al., 2015).

The GCS-ss-PEI/DNA nanoparticles were pseudo-spherical and well dispersed without aggregation as shown in Fig. 4-c. The median size of the polyplexes at N/P ratio of (20/1) was around 45 nm ($P < 0.05$), approximately the size that was determined by the Zeta potentiometer.

The stronger binding of cationic polymer to its encapsulated gene is a prerequisite for the gene vector. Agarose gel electrophoresis was employed to investigate the ability of HMW PEI and GCS-ss-PEI polycations to condense DNA at various N/P ratios ranging from 1 to 40 (Fig. 5a–b). There was no UV-intense bond at N/P ratios ≥ 1 observed for GCS-ss-PEI that showed highly efficient DNA condensation for GCS-ss-PEI (Fig. 5-a). In contrast, visible strips were found in an agarose gel electrophoresis image of HMW PEI at N/P ratios 1 and 2 (Fig. 5-b). The Branched LMW PEI that was incorporated into the structure of GCS-ss-PEI with branched PEI, and compared to linear PEI, has stronger complexation with DNA as it typically results in smaller complexes (Feng et al., 2014; Wightman et al., 2001). Redox-responsible characteristic of the GCS-ss-PEI was examined by agarose gel electrophoresis. A 10 mM

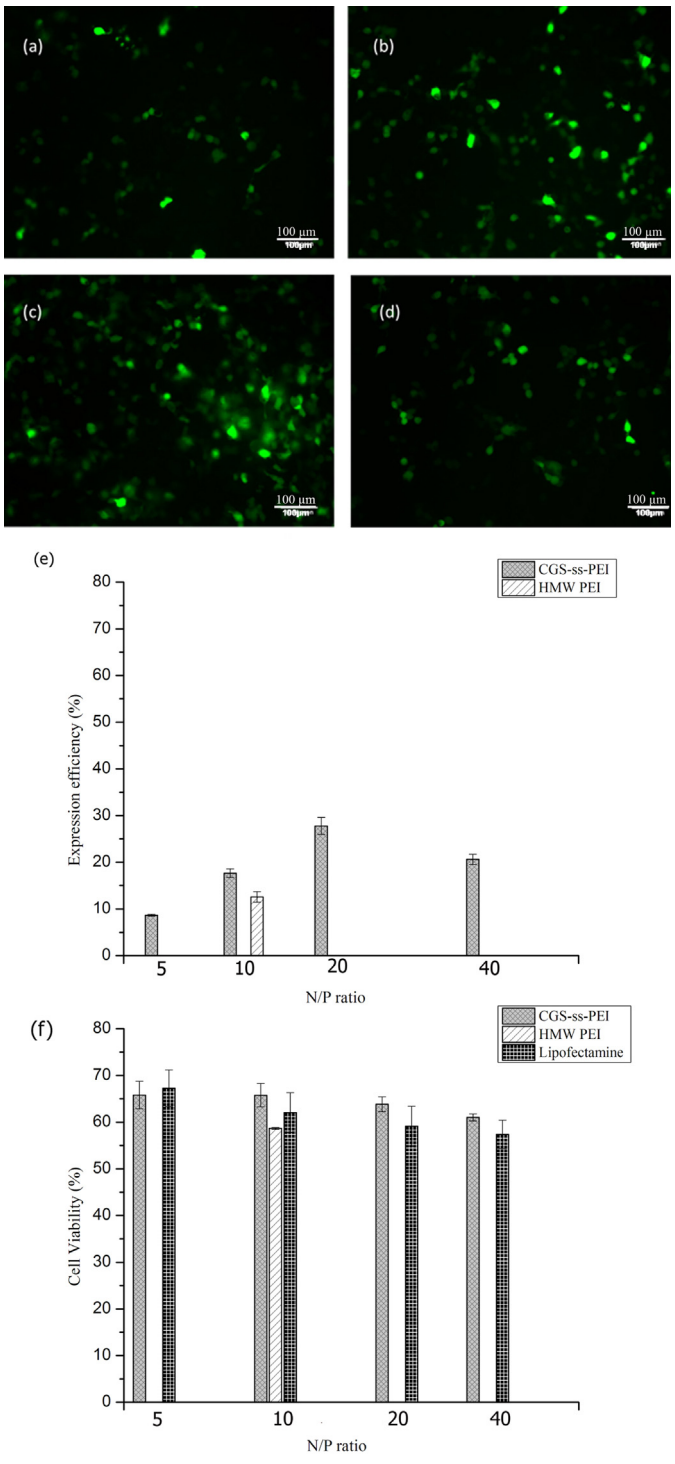

Fig. 7. Transfection efficiency of polyplexes in HEK 293 at different N/P ratios: GCS-ss-PEI/GFP DNA at N/P ratios of 5 (a), 10 (b), 20 (c) and HMW PEI/GFP DNA complex at the optimized N/P ratio of 10(d) HEK 293T cells. The flow cytometry assessment results (e) and cell viability (f) of GCS-ss-PEI, Lipofectamine®2000 at different N/P ratio (5–40) and HMW-PEI at N/P ratio 10.

GSH solution in the presence of heparin was employed to mimic cytosol microenvironment conditions. According to Fig. 5-c for no GSH condition, no DNA release was found from the polyplexes, which indicated the ability of GCS-ss-PEI to effectively support the entrapped gene. However, incubation of GCS-ss-PEI in GSH/heparin solution resulted in DNA release from polyplexes into the gel. GSH can cleave the disulfide bonds of GCS-ss-PEI into its fractures, gly-

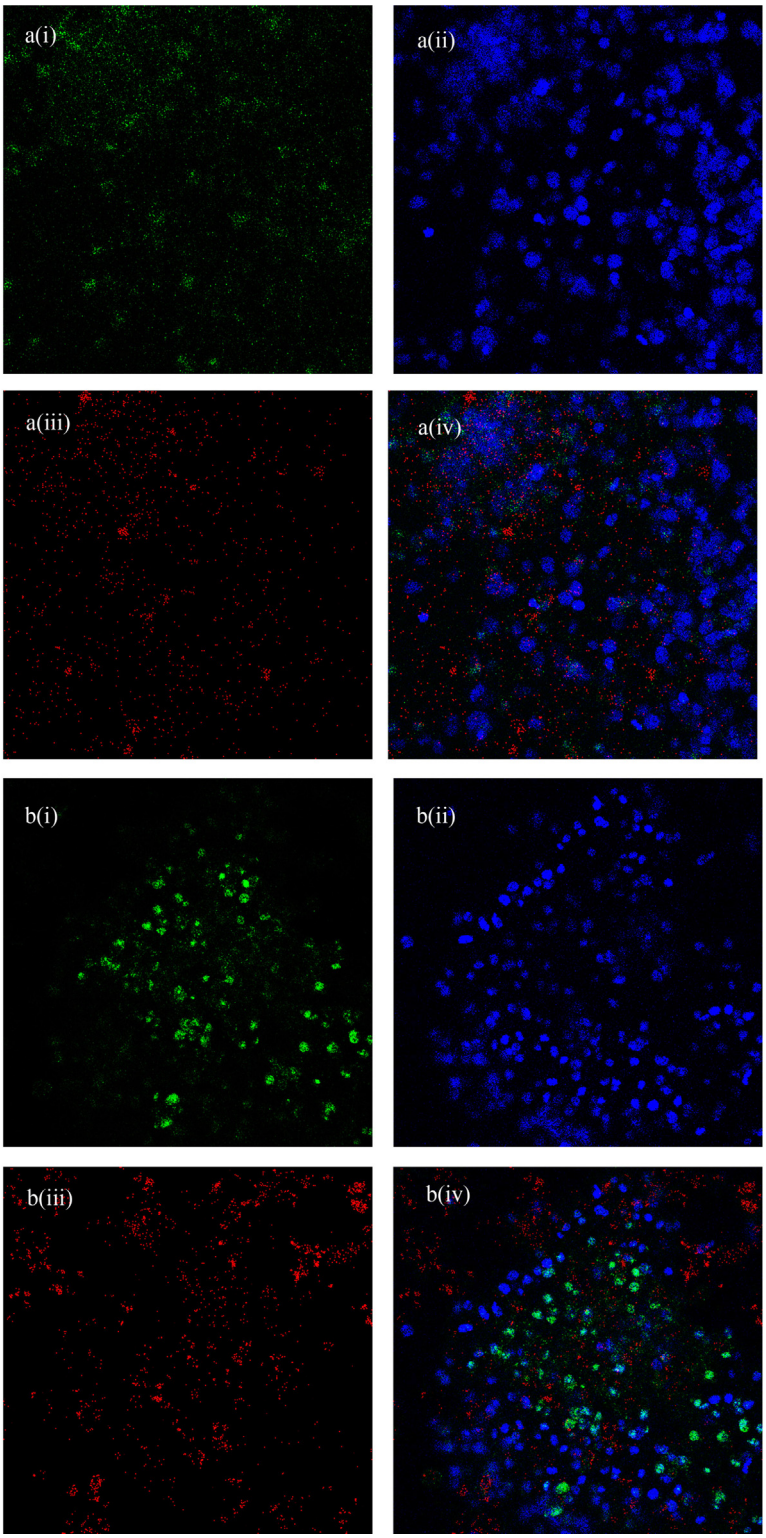

Fig. 8. Fig. 4. CLSM images of the intracellular localization of the FITC-labeled polyplexes loading pDNA (green) against HEK 293 cells at an N/P ratio of 10 (a (i–iv) HMW PEI, b (i–iv) GCS-SS-PEI). The late endosomes/lysosomes (red) and nuclei (blue) were stained with LysoView™ and DAPI, respectively (For interpretation of the references to colour in this figure legend, the reader is referred to the web version of this article.).

col chitosan and LMW-PEI, with relatively lower DNA condensation ability (Chumakova et al., 2008; Park et al., 2013; Xu, Zhang, Liu, & Zhang, 2013).

Due to the lower amount of positive charge per molecule, small PEIs cannot appropriately condense negatively charged DNA molecules. The branched PEI showed stronger complexation with DNA, as it typically resulted in smaller complexes (Feng et al., 2014; Wightman et al., 2001). This GSH-induced degradation of disulfide bonds can facilitate DNA release from GCS-ss-PEI in the presence of heparin. The GCS-ss-PEI cationic polymer with incorporated disulfide bonds effectively protected DNA from degradation and also was

able to release the entrapped DNA into a GSH/Heparin solution that mimics the reduced intracellular environment (Feng et al., 2014).

3.3. Cytotoxicity of GCS-ss-PEI

Fig. 6 shows the cytotoxicity of the polycations, evaluated in HEK 293 T cells by MTT assays at varying concentrations from 1 μg/ml to 1000 μg/ml of buffer media. For each type of carrier, the IC50 value, corresponding to the concentration of polymer at which 50% of the cells remained viable, was determined. There was a significant correlation between the concentration of the polycations and the cell viability ($P < 0.05$). GCS-ss-PEI showed the lowest toxicity ($P < 0.001$, with IC50 = 434.4 ± 45.7 μg/ml) in employed polymers when compared with LMWPEI ($P < 0.001$) and HMW PEI ($P < 0.045$), with IC50 values 262.4 ± 30.2 μg/ml and 27.1 ± 2.2 μg/ml, respectively. It has been reported that HMW PEI is significantly more toxic than LMW PEI, which is directly related to the polymer MW and its non-biodegradable structure (Urban-Klein, Werth, Abuharbeid, Czubayko, & Aigner, 2005).

In comparison with the high toxicity of HMW PEI, employing GCS NPs for gene delivery applications is not associated with significant toxicity (Kunath, von Harpe, Fischer, & Kissel, 2003; Makhlof et al., 2010; Mitra et al., 2014). Further, there was no systemic toxicity reported for the GCS-based gene carrier (Yhee et al., 2015). The GSH-cleavable structure of GCS-ss-PEI promoted its biodegradability and significantly reduced the level of cytotoxicity. The lower toxicity arises due to the reduction in the number of disulfide linkages, which enhanced the disassembly rate for catiomer-nucleic acid complexes. Moreover, a sharp drop in molecular weight of the catiomer, due to disulfide cleavage, resulted in lower toxicity (Taranejoo et al., 2015).

3.4. Gene transfection

Transfection of GCS-ss-PEI was qualitatively assessed at different N/P ratios (5, 10, 20) and compared with the transfection activity of commercial HMW PEI (at an N/P ratio of 10 as the optimum N/P ratio) using a fluorescence microscope. As shown in Fig. 7(a–d), the density of fluorescent cells after exposure to GCS-ss-PEI was far more obvious in comparison to the case of PEI (Zhao et al., 2013). The highest fluorescence was achieved when employing GCS-ss-PEI at N/P ratio 20. Fig. 7-e illustrates flow cytometry assessment results of GCS-ss-PEI at different N/P ratios (5–40) and HMW-PEI at N/P ratio 10. The transfection efficiency of GCS-ss-PEI was significantly higher compared to that of HMW PEI. The higher cell uptake of GCS-ss-PEI was due to its great buffering capacity and hence endosomal escape along with enhanced GFP DNA condensation ability. The increased transfection efficiency of polyplexes has been attributed to efficient endosomal escape (Chan et al., 2014).

Moreover, the facilitated GFP DNA release in cytosol, because of the intracellular GSH-induced cleavage of GCS-ss-PEI disulfide bonds, improved cell uptake. Interestingly, GCS-ss-PEI exhibited the highest transfection efficiency, (28.6 ± 2.8%), at an N/P ratio of 20. The transfection efficiency of GCS-ss-PEI decreased by increasing the N/P ratio from 20 to 40, indicating the saturation of the nanoparticles with GFP DNA while increasing toxicity (Jain, Kumar, Agrawal, Thankia, & Banerjee, 2015; Yu, Wu, & Li, 2016; Zhao et al., 2013). Cells viability values of GCS-ss-PEI based polyplexes at different N/P ratio (1–40) were compared with DNA complexes of Lipofectamine™2000, as a low toxic commercially available transfection reagent (Fig. 7-f) (Cui et al., 2012; L. Li et al., 2015; L.M. Li et al., 2015). There was no significant difference between the cell viability of GCS-ss-PEI and Lipofectamine™2000 polyplexes ($P > 0.055$). The cell survival rate slightly decreased by increasing N/P ratio from 5 to 40. However, the reduction was not significant ($P > 0.055$) confirming the correlation between N/P ratios and transfection efficiency results for GCS-ss-PEI polyplexes.

3.5. Endosomal escape

The intracellular localization of the polyplexes after cellular transfection was studied using confocal laser scanning microscopy (CLSM) to evaluate the endosomal escape capability.

GCS-ss-PEI polyplexes demonstrated significantly higher co-localization and hence endosomal escape compared to HMW PEI (Fig. 8 (a-b)). The major part of GCS-ss-PEI polyplexes was transferred to cytoplasm whereas a significant portion of GCS-ss-PEI polyplexes was localized in the late endosomes/lysosomes. These results had a good agreement with buffering capacity and gene transfection efficiency studies (Dominska & Dykxhoorn, 2010; Zha, Li, & Ge, 2015). The GCS-ss-PEI polyplexes presented higher gene transfection efficiency due to more efficient endosomal escape.

4. Conclusions

A new gene vector, GCS-ss-PEI, was fabricated by grafting PEI on glycol chitosan chains via bio-cleavable disulfide bonds. Utilizing GCS-ss-PEI produced a gene vector consisting of very small nanoparticles (less than 100 nm) of a pseudo-spherical shape with excellent dispersion without aggregation. The GCS-ss-PEI expressed good DNA binding efficiency, and redox-responsive characteristics, along with significantly reduced toxicity for model cells, HEK 293T, compared to commercial HMW PEI. Moreover, the transfection efficiency of GCS-ss-PEI was higher than for HMW PEI at the same N/P ratios that is attributed to more endosomal escape capability of GCS-ss-PEI. In sum, this novel gene vector is very promising as a potential vector for gene therapy.

Acknowledgement

The funding support of this research was provided by the Australian Research Council Discovery Grant DP130100822 and the Monash Institute of Medical Engineering(MIME). Specialized research advice by Dr. Charles Ma, Faculty of Medical Medicine, Nursing and Health Sciences, Monash University, for GFP DNA extraction is greatly appreciated.

References

Alamdarnejad, G., Sharif, A., Taranejoo, S., Janmaleki, M., Kalaee, M. R., Dadgar, M., et al. (2013). Synthesis and characterization of thiolated carboxymethyl chitosan-graft-cyclodextrin nanoparticles as a drug delivery vehicle for albendazole. *Journal of Materials Science: Materials in Medicine*, *24*(8), 1939–1949.

Cai, G., Conley, S., & Naash, M. (2008). Nanoparticle applications in ocular gene therapy. *Vision Research*, *48*(3), 319–324.

Chan, C. L., Majzoub, R. N., Shirazi, R. S., Ewert, K. K., Chen, Y. J., Liang, K. S., et al. (2014). Endosomal escape and transfection efficiency of PEGylated cationic liposome–DNA complexes prepared with an acid-labile PEG-lipid. *Biomaterials*, *33*(19), 4928–4935.

Chumakova, O. V., Liopo, A. V., Andreev, V. G., Cicenaite, I., Evers, B. M., Chakrabarty, S., et al. (2008). Composition of PLGA and PEI/DNA nanoparticles improves ultrasound-mediated gene delivery in solid tumors in vivo. *Cancer Letters*, *261*(2), 215–225.

Cui, S., Zhang, S., Chen, H., Wang, B., Zhao, Y., & ZHi, D. (2012). The mechanism of lipofectamine 2000 mediated transmembrane gene delivery. *Engineering*, *4*(10B), 172–175.

Dominska, M., & Dykxhoorn, D. M. (2010). Breaking down the barriers: siRNA delivery and endosomal escape. *Journal of Cell Science*, *123*(8), 1183–1189.

El-Sayed, A., Futaki, S., & Harashima, H. (2009). Delivery of macromolecules using arginine-rich cell-penetrating peptides: Ways to overcome endosomal entrapment. *AAPS Journal*, *11*(1), 13–22.

Feng, L., Xie, A., Hu, X., Liu, Y., Zhang, J., Li, S., et al. (2014). A releasable disulfide carbonate linker for polyethyleneimine (PEI)-based gene vectors. *New Journal of Chemistry*, *38*(11), 5207–5214.

Goula, D., Remy, J. S., Erbacher, P., Wasowicz, M., Levi, G., Abdallah, B., et al. (1998). Size, diffusibility and transfection performance of linear PEI/DNA complexes in the mouse central nervous system. *Gene Therapy*, *5*(5), 712–717.
Inbaraj, B. S., Tsai, T., & Chen, B. H. (2012). Synthesis, characterization and antibacterial activity of superparamagnetic nanoparticles modified with glycol chitosan. *Science and Technology of Advanced Materials*, *13*(1).
Jain, S., Kumar, S., Agrawal, A. K., Thankia, K., & Banerjee, U. C. (2015). Hyaluronic acid-PEI-cyclodextrin polyplexes: Implications for in vitro and in vivo transfection efficiency and toxicity. *RSC Advances*, *5*(51), 41144–41154.
Jia, L., Li, Z., Zhang, D., Zhang, Q., Shen, J., Guo, H., et al. (2013). Redox-responsive catiomer based on PEG-ss-chitosan oligosaccharide-ss-polyethylenimine copolymer for effective gene delivery. *Polymer Chemistry*, *4*(1), 156–165.
Kim, J. H., Kim, Y. S., Park, K., Lee, S., Nam, H. Y., Min, K. H., et al. (2008). Antitumor efficacy of cisplatin-loaded glycol chitosan nanoparticles in tumor-bearing mice. *Journal of Controlled Release*, *127*(1), 41–49.
Kunath, K., von Harpe, A., Fischer, D., & Kissel, T. (2003). Galactose-PEI-DNA complexes for targeted gene delivery: Degree of substitution affects complex size and transfection efficiency. *Journal of Controlled Release*, *88*(1), 159–172.
Li, L., Wei, Y., & Gong, C. (2015). Polymeric nanocarriers for non-viral gene delivery. *Journal of Biomedical Nanotechnology*, *11*(5), 739–770.
Li, L., Ruana, G., HuangFua, M., Chena, Z., Liu, H., Li, L., Hu, Y., et al. (2015). ScreenFect A: An efficient and low toxic liposome for gene delivery to mesenchymal stem cells. *International Journal of Pharmaceutics*, *488*(1–2), 1–11.
Lai, W. F. (2015). Microfluidic methods for non-viral gene delivery. *Current Gene Therapy*, *15*(1), 55–63.
Lu, H., Dai, Y., Lv, L., & Zhao, H. (2014). Chitosan-graft-polyethylenimine/DNA nanoparticles as novel non-viral gene delivery vectors targeting osteoarthritis. *Public Library Of Science*, *9*(1).
Makhlof, A., Werle, M., Tozuka, Y., & Takeuchi, H. (2010). Nanoparticles of glycol chitosan and its thiolated derivative significantly improved the pulmonary delivery of calcitonin. *International Journal of Pharmaceutics*, *397*(1–2), 92–95.
Mitra, R. N., Han, Z., Merwin, M., Al Taai, M., Conley, S. M., & Naash, M. I. (2014). Synthesis and characterization of glycol chitosan DNA nanoparticles for retinal gene delivery. *ChemMedChem*, *9*(1), 189–196.
Moyuan, C., Haixia, J., Weijuan, Y., Peng, L., Liqun, W., & Hongliang, J. (2012). A convenient scheme for synthesizing reduction-sensitive chitosan-based amphiphilic copolymers for drug delivery. *Journal of Applied Polymer Science*, *123*(5), 3137–3144.
Naldini, L. (2015). Gene therapy returns to centre stage. *Nature*, *526*(7573), 351–360.
Park, S. C., Nam, J. P., Kim, Y. M., Kim, J. H., Nah, J. W., & Jang, M. K. (2013). Branched polyethylenimine-grafted-carboxymethyl chitosan copolymer enhances the delivery of pDNA or siRNA in vitro and in vivo. *International Journal of Nanomedicine*, *8*, 3663–3677.
Patnaik, S., & Gupta, K. C. (2013). Novel polyethylenimine-derived nanoparticles for in vivo gene delivery. *Expert Opinion on Drug Delivery*, *10*(2), 215–228.
Ragusa, A., GarcÍa, I., & PenadÉs, S. (2007). Nanoparticles as nonviral gene delivery vectors. *IEEE Transactions on Nanobioscience*, *6*(4), 319–330.
Richard, I., Thibault, M., De Crescenzo, G., Buschmann, M. D., & Lavertu, M. (2013). Ionization behavior of chitosan and chitosan-DNA polyplexes indicate that chitosan has a similar capability to induce a proton-sponge effect as PEI. *Biomacromolecules*, *14*(6), 1732–1740.
Taghizadeh, B., Taranejoo, S., Monemian, S. A., Salehi Moghaddam, Z., Daliri, K., Derakhshankhah, H., et al. (2015). Classification of stimuli-responsive polymers as anticancer drug delivery systems. *Drug Delivery*, *22*(2), 145–155.
Taranejoo, S., Liu, J., Verma, P., & Hourigan, K. (2015). A review of the developments of characteristics of PEI derivatives for gene delivery applications. *Journal of Applied Polymer Science*, *132*(25).
Urban-Klein, B., Werth, S., Abuharbeid, S., Czubayko, F., & Aigner, A. (2005). RNAi-mediated gene-targeting through systemic application of polyethylenimine (PEI)-complexed siRNA in vivo. *Gene Therapy*, *12*(5), 461–466.
Wang, F., Liu, P., Nie, T., Wei, H., & Cui, Z. (2013). Characterization of a polyamine microsphere and its adsorption for protein. *International Journal of Molecular Sciences*, *14*(1), 17–29.
Wightman, L., Kircheis, R., Rössler, V., Carotta, S., Ruzicka, R., Kursa, M., et al. (2001). Different behavior of branched and linear polyethylenimine for gene delivery in vitro and in vivo. *Journal of Gene Medicine*, *3*(4), 362–372.
Xiaoxiao, G., Baoji, D., Yunhui, L., Ying, G., Dan, L., & Erkang, W. (2015). Vectors based on nanomaterials for gene delivery. *Progress in Chemistry*, *27*(8), 1093–1101.
Xu, Z., Zhang, K., Liu, X., & Zhang, H. (2013). A new strategy to prepare glutathione responsive silica nanoparticles. *RSC Advances*, *3*(39), 17700–17702.
Yhee, J. Y., Song, S., Lee, S. J., Park, S. G., Kim, K. S., Kim, M. G., et al. (2015). Cancer-targeted MDR-1 siRNA delivery using self-cross-linked glycol chitosan nanoparticles to overcome drug resistance. *Journal of Controlled Release*, *198*, 1–9.
Yin, H., Kanasty, R. L., Eltoukhy, A. A., Vegas, A. J., Dorkin, J. R., & Anderson, D. G. (2014). Non-viral vectors for gene-based therapy. *Nature Reviews Genetics*, *15*(8), 541–555.
Yu, K., Wu, S., & Li, H. (2016). A chitosan-graft-PEI-eprosartan conjugate for cardiomyocyte-targeted VEGF plasmid delivery in myocardial ischemia gene therapy. *Journal of Experimental Nanoscience*, *11*(2), 81–96.
Yue, J., Wu, J., Liu, D., Zhao, X., & Lu, W. W. (2015). BMP2 gene delivery to bone mesenchymal stem cell by chitosan-g-PEI nonviral vector. *Nanoscale Research Letters*, *10*(1).
Zha, Z., Li, J., & Ge, Z. (2015). Endosomal-escape polymers based on multicomponent reaction-synthesized monomers integrating alkyl and imidazolyl moieties for efficient gene delivery. *ACS Macro Letters*, *4*(10), 1123–1127.
Zhang, S., & Cahalan, M. D. (2007). Purifying plasmid DNA from bacterial colonies using the qiagen miniprep kit. *Journal of Visualized Experiments*, *6*.
Zhang, Q. F., Yi, W. J., Wang, B., Zhang, J., Ren, L., Chen, Q. M., et al. (2013). Linear polycations by ring-opening polymerization as non-viral gene delivery vectors. *Biomaterials*, *34*(21), 5391–5401.
Zhao, X., Li, Z., Pan, H., Liu, W., Lv, M., Leung, F., et al. (2013). Enhanced gene delivery by chitosan-disulfide-conjugated LMW-PEI for facilitating osteogenic differentiation. *Acta Biomaterialia*, *9*(5), 6694–6703.